Perspective

Lattice metamaterials as advanced airborne sound insulators

Xinwei Li,[1,*] Xinxin Wang,[2] Miao Zhao,[3] and Zhendong Li[2,4]

[1] *Newcastle University in Singapore, Faculty of Science, Agriculture, and Engineering, Newcastle University, Newcastle upon Tyne NE1 7RU, UK*

[2] *School of Traffic & Transportation Engineering, Central South University, Changsha 410075, Hunan, China*

[3] *School of Mechanical and Electrical Engineering, University of Electronic Science and Technology of China, Sichuan 611731, China*

[4] *Department of Mechanical Engineering, National University of Singapore, Singapore 117576, Singapore*

(Received 30 June 2025; revised 21 September 2025; published 11 December 2025)

This paper is a contribution to the Physical Review Applied collection titled Phononics and Metamaterials.

Airborne sound insulation is vital for noise reduction across various engineering fields. Traditional mass-based soundproofing methods, while effective, are often hindered by their bulkiness and limited ventilation capability. In contrast, lattice metamaterials provide a lightweight architected alternative with high tunability, enabling the use of periodic geometries to manipulate sound through mechanisms such as Bragg scattering and local resonance. This perspective explores the acoustic capabilities of various lattice morphologies, offers preliminary recommendations on geometry selection for effective sound insulation, and presents a generalized analytical model for predicting sound transmission loss. We also present a forward-looking discussion on the unbounded design potential of lattice topologies, highlighting opportunities for multifunctionality and outlining future directions in smart design, adaptive lattice structures, and data-driven optimization to enable advanced noise control and the development of multifunctional metamaterials.

DOI: 10.1103/2w5x-vh9f

I. INTRODUCTION

Airborne noise, commonly regarded as a disruptive form of pollution, presents challenges in both residential and industrial environments. It can impact on human comfort, health, and productivity, and also hinders the performance of sensitive equipment and systems. As a result, effective airborne sound insulation is vital across diverse engineering applications, from building design and transportation to industrial machinery, where controlling sound transmission is essential for both occupant well-being and system reliability. Conventional soundproofing approaches have historically relied on the use of dense and bulky materials, adhering to the classical mass law, which states that increasing the mass of a barrier leads to improved sound attenuation [1]. However, modern applications increasingly demand barriers that are lightweight and permit effective ventilation for heat dissipation and air exchange, highlighting the need for innovative alternatives to conventional dense materials.

To address these limitations, efforts in airborne-sound-insulating materials have focused on periodic architectured materials, engineered as sonic crystals, as a promising class of sound insulators [2,3]. Unlike traditional materials, sonic crystals utilize wave-based mechanisms such as Bragg scattering and local resonance to manipulate acoustic wave propagation, enabling sound attenuation across targeted and subwavelength regimes. Some typical sonic crystal configurations include arrays of cylinders [4], cylindrical features of complex cross sections [5], spheres, and shapes [6], or even naturally occurring features such as arrays of trees [7]. Advanced metadesigns incorporate hollow features with perforations [8] or hierarchical structures [9,10] that additionally introduce local resonance, enabling sound attenuation at subwavelength frequencies that are difficult to address with Bragg scattering alone. The design flexibility and tunability of sonic crystals make them a powerful tool for controlling airborne sound in a wide range of applications, including architectural acoustics, transportation, and ventilation systems. Therefore, sonic crystals are widely adopted in real life along transportation corridors [2], buildings, to serve as sound barriers that are also air ventilating and aesthetically pleasing [11,12].

*Contact author: xinwei.li@newcastle.ac.uk

Published by the American Physical Society under the terms of the Creative Commons Attribution 4.0 International license. Further distribution of this work must maintain attribution to the author(s) and the published article's title, journal citation, and DOI.

Among the various types of periodic architecture materials, lattice metamaterials stand out due to their geometric versatility and the richness of their design space [13–15]. Lattice metamaterials are porous three-dimensional structures composed of repeating unit-cell topologies formed by struts, shells, plates, or combinations of these elements. Variation in lattice topology imparts the ability to tailor and achieve distinct physical properties. At present, lattice metamaterials have been widely adopted for applications as lightweight structures [16], energy absorbers [17], sound absorbers [15,18,19], thermal metamaterials [20], and electromagnetic metamaterials [21], to name a few. With control over intrinsic parameters such as topology and relative density, as well as extrinsic factors such as unit-cell size and assembly [15], we foresee lattice metamaterials as a highly tunable platform for targeted airborne sound control. Their inherent structural architecture also enables seamless integration with additional functional requirements, thereby expanding their potential as multifunctional sound insulators. Despite this, the potential of lattice metamaterials for sound insulation remains insufficiently explored, highlighting the need for investigations to elucidate and leverage their capabilities in this domain.

In this perspective, we examine the potential and advocate lattice metamaterials as advanced airborne sound insulators. This perspective first provides a brief introduction to lattice structures, proposed mechanisms behind sound attenuation in lattice structures, structural-property relationships, and analytical modeling approaches. It then highlights emerging opportunities for lattice metamaterials to function not only as sound insulators but also as multifunctional materials with combined mechanical, thermal, and electromagnetic capabilities, paving the way for next-generation solutions in noise control and beyond.

II. LATTICE STRUCTURES

A. Topology

Lattice structures are three-dimensional periodic architectures composed of repeating unit cells that can be tailored with virtually unlimited potential in geometric variations [22]. These architected materials are commonly categorized into three primary topological classes (Fig. 1), truss, TPMS (triply periodic minimal surface), and plate, each defined by their fundamental structural motifs, with a fourth category encompassing hybrid structures that integrate one or more features from the other three. Truss lattices consist of struts joined at nodes, often inspired by Bravais-crystal geometries such as simple cubic (sc), body-centered cubic (bcc), or face-centered cubic (fcc) arrangements [23]. TPMS lattices are based on smooth continuous shells with zero mean curvature, such as the gyroid, diamond, or primitive surfaces, and can exist in both shell-like and skeletal forms depending on whether the surface or its void space is retained [24]. Plate lattices,

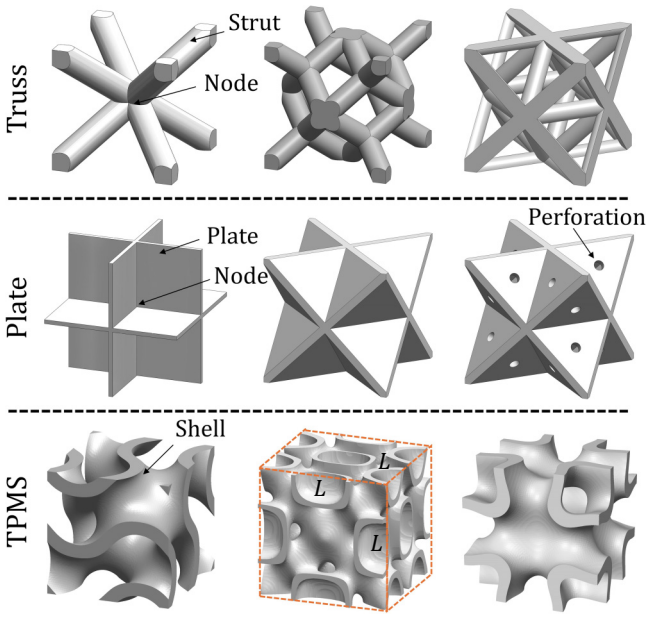


FIG. 1. An overview of the various types of lattice metamaterials.

a more recent innovation, are composed of flat plate elements arranged in a periodic and strategic manner [25,26]. To address manufacturing constraints associated with powder-bed fusion and vat-photopolymerization additive manufacturing techniques, perforations are often introduced at specific locations on the closed-cell plates, such as nodal or face regions, for the removal of feedstock material. Hybrid lattices combine different structural motifs of the previously mentioned types of lattices [27,28], either within a single unit cell or across spatially varying arrangements, enabling tailored physical properties or to achieve multifunctionality. Despite the vast range of possible designs, lattice structures can be fundamentally defined by two intrinsic parameters: morphology, which captures the geometric form, and relative density, which quantifies the solid-volume fraction within a unit cell. For example, as schematically illustrated in Fig. 1, relative density is defined as the ratio of the solid volume of the lattice to the total volume of its bounding cube ($L \times L \times L$). It ranges from 0, representing nothing, to 1, representing a fully solid material. Additional descriptors such as unit-cell size and repetition are considered to be extrinsic and may pose an influence on scale-dependent behaviors. Together, these factors offer a versatile design space for achieving customizable physical properties and render them ideal for engineering Bragg scattering and local resonant features to allow targeted airborne-sound attenuation.

B. Attenuation mechanisms

Based on existing research on acoustic metamaterials, we foresee sound insulation in periodic lattice structures to

be primarily governed by two physical mechanisms: Bragg scattering and local resonance [29–32].

Bragg scattering represents the primary mechanism of sound attenuation in periodic structures and is intrinsically linked to any form of periodicity, including that found in lattice architectures. This phenomenon arises from the interaction, particularly scattering, of incident sound waves and the periodic geometry of the material, resulting in constructive- and destructive-interference patterns. With sufficient sound-wave scattering and in the right conditions, particularly a wavelength twice the size of the lattice periodicity, destructive interference leads to the formation of phononic band gaps, effectively blocking sound transmission at that frequency. Mathematically, the Bragg resonant frequency, f_b, can be predicted using the sound speed through the transmitting medium, c, and the unit-cell size, or periodicity, L, via

$$f_b = \frac{c}{2L} \quad . \tag{1}$$

This geometry-dependent mechanism enables predictable and tunable acoustic attenuation based solely on the lattice periodicity, which is the size.

Differing from Bragg scattering, local resonance mechanisms [33], such as Helmholtz, structural, Fabry-Perot, Fano, or membrane resonance, offer structure-specific attenuation at subwavelength frequencies. Local resonance leverages metamaterial architecture that incorporates resonant elements such as perforations, cavities, or membranes that resonate at specified frequencies [29,30,34]. In terms of lattice structures, the most probable and relevant local resonance mechanisms would be structural resonance and Helmholtz resonance. Helmholtz resonance occurs with a narrow neck (or pore) and large cavity morphology, where a mass-spring damper system arises, with the oscillating air in the neck acting as a mass and the compressible air in the cavity acting as a spring. When excited at the resonant frequency, this configuration produces pressure oscillations within the cavity that trap acoustic energy and attenuate transmitted sound via thermal and viscous dissipation in boundary layers. The resonant frequency can be tuned by adjusting geometric parameters such as the pore diameter, pore depth, and cavity volume, to be discussed in greater detail in Sec. IV. Structural resonance, in contrast, refers to resonance that arises from standing-wave formation within the internal volume of a cavity. They typically form when its dimensions support quarter- or half-wavelength modes, leading to the entrapment and scattering of acoustic energy. Because local resonance does not require periodicity on the scale of the acoustic wavelength, it allows lattice structures to achieve subwavelength band gaps—a key advantage in designing thin and lightweight highly attenuating sound insulators. Moreover, being periodic, lattice can simultaneously harness both Bragg scattering and local resonance to broaden attenuation bandwidth and increase effectiveness across different frequency ranges.

III. STRUCTURAL-PROPERTY RELATIONSHIPS

Based on their acoustic behavior, lattice structures may be broadly categorized into two types: (i) plate and TPMS-based lattices, which exhibit large acoustic contrast and can support both Bragg scattering and local resonance, and (ii) truss-based lattices, which feature slender struts with minimal acoustic impedance contrast and limited sound-insulation capability.

Plate lattices and TPMS structures feature continuous high coverage of solid surfaces or curves that introduce significant acoustic impedance mismatch with air, which leads to stronger scattering and reflection [35]. Since Bragg scattering relies on periodic reflection of sound waves, Bragg scattering is thus stronger in plate and TPMS lattices. This is true regardless of the material used to fabricate the lattice metamaterial, considering the acoustic impedance of any elastomer, polymer, or metal, to be much higher, in the ranges of 10^6–10^7 Pa s m^{-1}, compared to the air at 415 Pa s m^{-1}. This trend is evident in the sound-transmission loss (STL) plots in Figs. 2(a)–2(d), which display the frequency-dependent STL curve, expressed in decibels (dB), for several representative lattice structures, modeled through finite-element analysis. The corresponding band diagrams are shown in the same figure, revealing band gaps that align with the frequencies of peak attenuation.

The acoustic modeling has been carried out in COMSOL MULTIPHYSICS, using the PRESSURE ACOUSTICS and THERMOVISCOUS ACOUSTICS modules. The model has replicated the experimental impedance-tube setup, with air modeled using built-in COMSOL parameters and the lattice solid assigned as a sound-hard boundary, a reasonable representation given the high impedance mismatch of solid materials with air [30]. The STL curves have been computed using the relation $\mathrm{STL} = 10\log_{10}(P_{\mathrm{in}}/P_{\mathrm{out}})$, with P_{in} and P_{out} obtained via surface integration of the acoustic pressures at the inlet and outlet, respectively. Band-structure analysis has been performed using Floquet periodic boundary conditions applied to the representative volume element of the lattice, scanning the k vector from [0 0 0] to [π/L 0 0] of the cubic symmetrical structures. All structures are modeled at a relative density of 30%, with a unit-cell size of 20 mm and three unit cells through the thickness. The evaluated lattices include the classic fcc plate—two versions, one with pore openings at the node and one at the face—the sc plate, which resembles a perforated sandwich panel, and the gyroid, a classical TPMS structure. For all designs, the Bragg frequency, calculated using Eq. (1), is 8575 Hz. Consistently, all structures exhibit transmission-loss spikes near this frequency. Notably, the fcc plate (face) [Fig. 2(b)] shows an additional

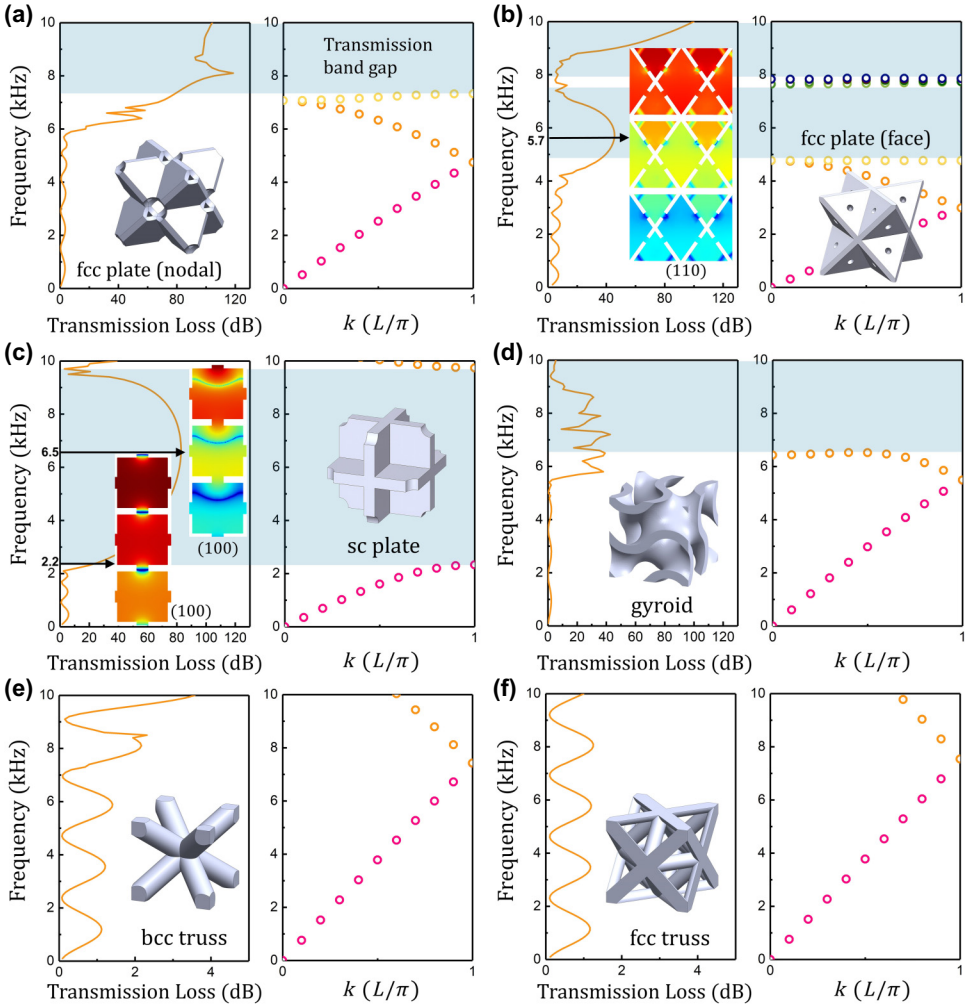


FIG. 2. The sound-transmission properties of various lattice metamaterials. FEA-modeled STL curves and the corresponding band diagrams: (a) fcc plate (nodal); (b) fcc plate (face); (c) sc plate; (d) gyroid; (e) bcc truss; (f) fcc truss. The insets in (b) and (c) reveal FEA-modeled SPL mapping across the selected plane of the lattice.

transmission gap, while the sc plate [Fig. 2(c)] presents a broadened attenuation peak, both attributable to the presence of additional local resonances within their architectures. In the insets of Figs. 2(b) and 2(c), we also show the sound-pressure plot (SPL), generated using the innate *ta.Lp* function in the THERMOVISCOUS ACOUSTICS module of COMSOL. For clarity, the SPL map of the fcc-plate (face) structure is presented along the (110) crystallographic cross section. The SPL distribution at 5700 Hz, nearing the transmission-loss maximum in the STL plot, reveals a clear signature of local resonance-induced attenuation within the perforated plate lattice. The SPL distribution at 5700 Hz in the lattice structure reveals clear evidence of local resonance phenomena. High sound-pressure levels are observed to be trapped within the octahedral cavities, with rapidly diminishing SPL regions observed at the pores, and diagonally near edges of the cavities, clear indication of local resonance-induced sound trapping [36]. This energy trapping leads to an impedance mismatch between the resonant zones and the surrounding medium, causing strong reflection and a sharp drop in the transmitted sound pressure beyond the resonant region. Figure 2(c) then reveals the SPL maps of the sc plate, observed at the (100) crystallographic planes. As observed, at low frequencies such as 2.2 kHz, the region of diminishing SPL around the necks of the structure suggests the acoustic response to be dominated by Helmholtz resonance. Indeed, the sc plate is reminiscent of a Helmholtz resonator, with the narrow pore behaving analogously to the "mass" in a Helmholtz-resonator model, while the adjacent cavity acts as the "spring." Energy is trapped near the neck and attenuation takes place from the viscous dissipation of sound energy. In contrast, at higher frequencies such as 6.5 kHz, the wavelength shortens, allowing the cavity to support more complex standing-wave patterns. As a result, the SPL concentration shifts from the neck toward the cavity center,

where pressure antinodes form. This indicates a transition to structural resonance, in which the shape and size of the internal cavity define the resonant behavior rather than Helmholtz resonance. For both structures, as the wave propagates downward through the subsequent slices, progressive drops in SPL are evident, transitioning from red and yellow (high SPL) to blue (low SPL), demonstrating strong suppression of transmitted sound. As observed, the resulting local resonant attenuation contributes to STL enhancement well below the Bragg range, offering a route to multiband noise reduction. Notably, in the work of Li *et al.*, a particular tubular and perforated fcc-plate cell has enabled additional local resonance, at a frequency of 1810 Hz, well below the calculated Bragg frequency at 8575 Hz [32].

In contrast, truss lattices are composed of slender struts interconnected at nodes. These struts, occupying a small fraction of the total volume, offer a sparse air gap and sound waves readily propagate through the void-dominated architecture with minimal interaction. Truss lattices thus offer low acoustic impedance relative to air with minimal wave scattering. As a result, Bragg scattering is weak or absent, and STL curves for such structures typically exhibit no distinct Bragg attenuation peaks. This is evident from the STL plots in Figs. 2(e) and 2(f). Similarly, no band gap has been shown in the frequency range of interest. Furthermore, local resonance is generally unattainable in truss lattices due to the lack of enclosed cavities or compliant resonant elements [18]. Unlike plate lattices that can be perforated to create Helmholtz resonators, truss lattices do not naturally support such features unless externally modified, such as plate-truss hybrids [26].

IV. ANALYTICAL SOLUTION

Since acoustic properties are based solely on geometry, structure-based analytical models can be proposed to model the sound-attenuation properties, in terms of the STL curve, of lattice structures. The model can be achieved by discretizing the geometry, particularly into a series of porous scatters along sound incidence, to achieve the overall acoustic impedance. Generally, acoustical analytical solutions are derived using the transfer-matrix method. The transfer matrix links the acoustic pressure, P, and velocity, U, on the inlet, at position $x = 0$, and outlet side, at position $x = N \times L$, of the lattice structure:

$$\begin{bmatrix} P \\ U \end{bmatrix}_{x=0} = T \begin{bmatrix} P' \\ U' \end{bmatrix}_{x=N\times L} . \tag{2}$$

Variables N and L refer to the number of unit cells along sound incidence and the unit-cell size, respectively. Since most lattices are cubic in nature, the total length for sound incidence across the lattice can be regarded as $N \times L$. T refers to the overall transfer matrix of the entire lattice.

We first look into the example of the transfer matrix of a cylindrical cavity. For a cylinder of radius r and cavity height D, the transfer matrix, T_C, can be given as

$$T_C = \begin{bmatrix} \cos(k_C D) & iZ_C \sin(k_C D) \\ \frac{i\sin(k_f D)}{Z_C} & \cos(k_C D) \end{bmatrix} . \tag{3}$$

Z_c refers to the normalized acoustic impedance of the cavity, given as

$$Z_c = \frac{\rho_0 c_0}{A_c} , \tag{4}$$

where A_c refers to the normal surface area of the geometry, e.g., πr^2 here, and ρ_0 and c_0 refer to the air density and speed of sound through air, respectively. k_0 refers to the complex wave number, given as by $k_0 = 2\pi f/c_0$, with f being the frequency.

While Eq. (3) can be used to calculate the effective transfer matrix of a standard structure, e.g., a cylindrical structure, it can also be generalized to any arbitrary shapes by discretization and effective radius. For example, in a structure where the radius r varies as a function of depth D, the profile can be discretized into infinitesimal slices, each with thickness D_i and radius r_i. This method has been shown with success in the work of Li *et al.* [32]. For each ith slice, the normalized acoustic impedance ($Z_{c,i}$), with respect to the area of each slice, $A_{c,i}$, can then be calculated as

$$Z_{c,i} = \frac{\rho_0 c_0}{A_{c,i}} . \tag{5}$$

The matrix for each layer can then be computed based on $Z_{c,i}$ and D_i of each slice:

$$T_{C,i} = \begin{bmatrix} \cos(k_0 D_i) & iZ_{C,i} \sin(k_0 D_i) \\ \frac{i\sin(k_0 D_i)}{Z_{C,i}} & \cos(k_0 D_i) \end{bmatrix} . \tag{6}$$

The overall transfer matrix T_C for the entire cavity can be obtained by successively multiplying the transfer matrices of all slices:

$$T_C = T_{C,1} T_{C,2} T_{C,3} \ldots \cdot T_{C,i},\ i \in \mathbb{Z}^+ . \tag{7}$$

With this, we can obtain the T_C for any geometry, e.g., narrow regions, large cavities, cavities of different shapes, etc.

Also, for the stacking of geometries, as a simple example, consider two successive cylindrical cavities with different diameters; we can simply apply the transfer-matrix method using Eq. (7) to account for the two cavities. For instance, considering the matrix for the two cylinders to be

T_{C1} and T_{C2}, the overall matrix, T, for the structure is then

$$T = T_{C1}T_{C2} \ . \tag{8}$$

For T, it is also in the form of

$$T = \begin{bmatrix} t_{11} & t_{12} \\ t_{21} & t_{22} \end{bmatrix} . \tag{9}$$

The overall normalized impedance, upon the exit from the lattice, is then

$$Z_L = \frac{\rho_0 c_0}{A_L} \ , \tag{10}$$

where A_L refers to $L \times L$. The STL value at each frequency, as the wave exits the structure, is then computed using the following expression:

$$\mathrm{STL} = 20\log_{10}\left|\frac{1}{2}\left(t_{11} + \frac{t_{12}}{Z_L} + Z_L t_{21} + t_{22}\right)\right| \ . \tag{11}$$

Subsequently, the sc-plate lattice as shown in Fig. 2(c) is employed to demonstrate the effectiveness of the analytical solution in accurately modeling the STL curve. The schematic of a three-layer sc plate is shown in Fig. 3(a), where the sketch is rendered translucent to reveal the internal lattice structure. Unlike the configuration shown in Fig. 2(c), here we apply a transposition to redefine the sc-plate unit cell, enabling a clearer visual illustration of the continuous cavity along the thickness direction for modeling purposes. Regardless, the overall lattice geometry is the same. As previously mentioned, the analytical model focuses on the geometry of the air phase rather than the solid lattice itself. Therefore, in Fig. 3(b)(i) we present the schematic of the inverse lattice, representing the air domain. Here, we can see the air phase of the sc plate to be approximated by repetitions of three distinct phases, as denoted on the same figure. Phase I, to obtain $T_{C,I}$, consists of the circular volume delineated by diameter d and thickness t_1. Phase II represents the cubic cavity approximated with edges of D, and phase III consists of the circular volume delineated by d and thickness t_2, where $t_2 = 2 \times t_1$. Thus, to compute the overall transfer matrix T_C, the three phases can be sequentially modeled by incorporating their respective geometries into the transfer-matrix framework, following the procedures detailed in Eqs. (2)–(11) and illustrated in Fig. 3(b)(ii). Here, d, t_1, D, and L correspond to 2, 1.2, 17.6, and 20 mm, respectively. In Fig. 3(c), we present a comparison between the analytically modeled and finite element analysis (FEA) simulated [the same with the one in Fig. 2(c)] STL curves of the sc plate. The close agreement observed validates the accuracy of our proposed analytical model. This highlights the effectiveness of our general geometry-based formulation for estimating STL using only lattice geometry as the input.

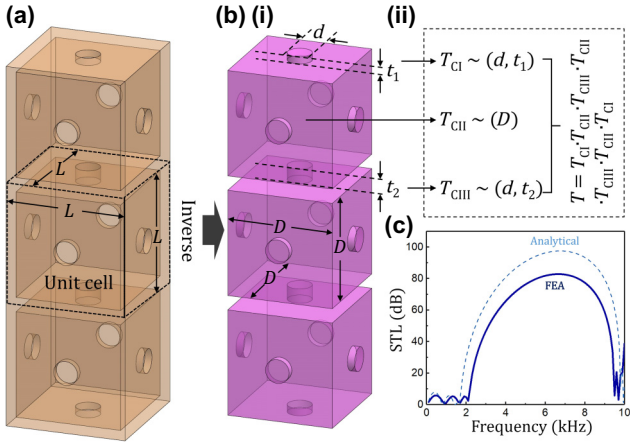


FIG. 3. Analytical modeling of the sc plate. (a) An illustration of a column of lattice, with three units through the thickness. (b) Illustrations of (i) the air geometry inside the lattice and (ii) the transfer matrix necessary to model the lattice. (c) A comparison of the analytical and FEA-modeled STL curves of the sc plate.

Here, we have presented a general geometry-based analytical formulation for estimating the STL based on just the lattice geometry as a starting point. For different lattice geometries, whether pores, cavities, or complex networks, the configuration of the air phase must be carefully discretized and characterized to accurately capture acoustic wave interactions.

V. FUTURE OUTLOOK

Thus far, this perspective has shown the emerging potential of lattice metamaterials as high-performance airborne sound insulators. By leveraging periodic architectures and geometry-driven acoustic phenomena, such as Bragg scattering and local resonance, lattice structures offer promising pathways to achieving broadband and subwavelength sound attenuation with significantly reduced mass and volume compared to conventional materials. This section will then explore the remarkable design flexibility of lattice metamaterials, their potential for multifunctional applications, and emerging innovations in structural concepts and design strategies.

A. Unbounded design potential

As detailed in Sec. II A, there are virtually unlimited design possibilities for lattice metamaterials. One of the most direct design levers is the freedom in topology to achieve local resonance. Helmholtz or structural resonance can be achieved by incorporating features such as perforations, cavities, or hollow features [29,30] amongst many. Such features can be easily achieved via targeted topological design or the hybridization of features. Even in the same topology, the resonant frequency can be finely tuned by modifying lattice geometric parameters such as

the plate or shell thickness, strut diameter, or deliberate pore introduction, such as in plate lattices. In parallel, the unit-cell size directly determines the onset of Bragg scattering [32]. This relationship allows engineers to tune the Bragg frequency by simply scaling the unit cell, making it possible to target specific frequency ranges of interest from mid- to high-frequency noise environments. Specifically, resonant frequencies halves with the doubling of cell size. In the work of Li *et al*., it is also reported that increasing the number of resonant layers does not shift the resonance frequency but instead enhances the attenuation intensity, providing further design control without compromising compactness [32]. Herein, our proposed analytical model proves to be an effective tool for accurately predicting STL and other effective acoustic properties of lattice structures, offering a geometry-driven approach that reduces reliance on complex simulations and experiments.

B. Multifunctionality

Beyond their acoustic performance, lattice structures exhibit exceptional multifunctionality, offering synergistic advantages in mechanical, thermal, and electromagnetic domains. This makes them attractive candidates for integrated systems in which multiple physical functions must be achieved simultaneously without added mass or volume. From a mechanical perspective, lattice architecture inherently delivers a high strength-to-weight ratio, owing to the low relative density and geometrically efficient load paths of lattice structures. Depending on the topology—whether truss, TPMS, or plate-based—lattices can be optimized for isotropy, stiffness, elastic modulus, or energy absorption, to name a few, allowing them to be ideal for applications as lightweight and/or protective materials. For instance, plate lattices have been shown to reach the Hashin-Shtrikman upper bounds for isotropic stiffness [25], while bending-dominated lattices such as bcc trusses offer a low strength with a high toughness for energy absorption [37]. By tuning just the lattice architecture, the mechanical response can be tailored without altering the overall material volume, offering precise control over mechanical properties and deformation modes. In Fig. 4(a)(i), we present a hybrid lattice structure exhibiting a pronounced plateau stress during deformation, indicative of strong energy-absorption capability. In turn, in Fig. 4(b), we display the cyclic compression stress-strain response of a lattice structure, highlighting its excellent deformation recoverability.

In addition to mechanical advantages, lattice structures are increasingly explored for their thermal properties. The porous nature of lattice structures allows them to serve as thermal insulators when being adapted in sandwich panels [38]. As shown in Fig. 4(b)(i), increasing the porosity of the lattice reduces its thermal conductivity, enabling tunable heat-transfer performance based on both porosity and material selection. By introducing anisotropy, it is also possible to control directional heat flow, offering a pathway toward thermal rectification or insulating layers that retain structural functionality [42]. Otherwise, if flow is involved, the high surface-area-to-volume ratio of lattice structures facilitates ventilation and the internal porosity can be tailored to induce pressure drop and promote forced convection, thereby enhancing thermal transport through both conduction and convection mechanisms [20]. For instance, in Fig. 4(b)(ii) we show the potential of various modified gyroid lattices capable of inducing very high pressure drop, high outlet velocity, and thus high convective heat-transfer coefficients [39]. The use of thermally conductive or insulating base materials can further augment their thermal role, depending on the application.

Electromagnetic wave absorption is another emerging frontier for lattice materials [21,43]. Unlike traditional solid materials, architected lattices offer unique advantages due to their geometric tunability. Features such as porosity and unit-cell architecture can be designed to improve impedance matching with air, allowing more electromagnetic waves to enter the material instead of reflecting off the surface of a bulk material [Fig. 4(c)]. Once inside, the waves experience multiple reflections and resonances within the structure, leading to effective attenuation [21]. These structures not only support efficient electromagnetic wave absorption but also offer excellent mechanical strength, making them highly suitable for multifunctional applications in aerospace and other advanced technologies.

C. Smart and hybrid design

Looking ahead, the future of lattice metamaterials in airborne sound insulation will likely move beyond passive architectures toward more adaptive, data-driven, and multifunctionally integrated systems. One promising direction involves the development of adaptive and active lattice structures, which incorporate stimuli-responsive materials based on environment, or properties such as piezoelectric, magnetorheological, and shape memory [44]. These active elements can dynamically alter the acoustic behavior of the lattice in response to environmental stimuli or user-defined inputs [45]. For example, shape-memory inclusions could modulate internal geometries under thermal activation, effectively tuning resonance frequencies in real time. Such systems pave the way for smart acoustic filters, reconfigurable noise barriers, and programmable metamaterials that adapt to varying operational needs, offering unprecedented control over sound propagation.

In parallel, novel design strategies are expected to revolutionize how lattice structures are conceived and optimized. By harnessing physics-informed inverse design principles, coupled with computational tools such as topology optimization, generative design, and machine-learning algorithms, it is possible to automatically

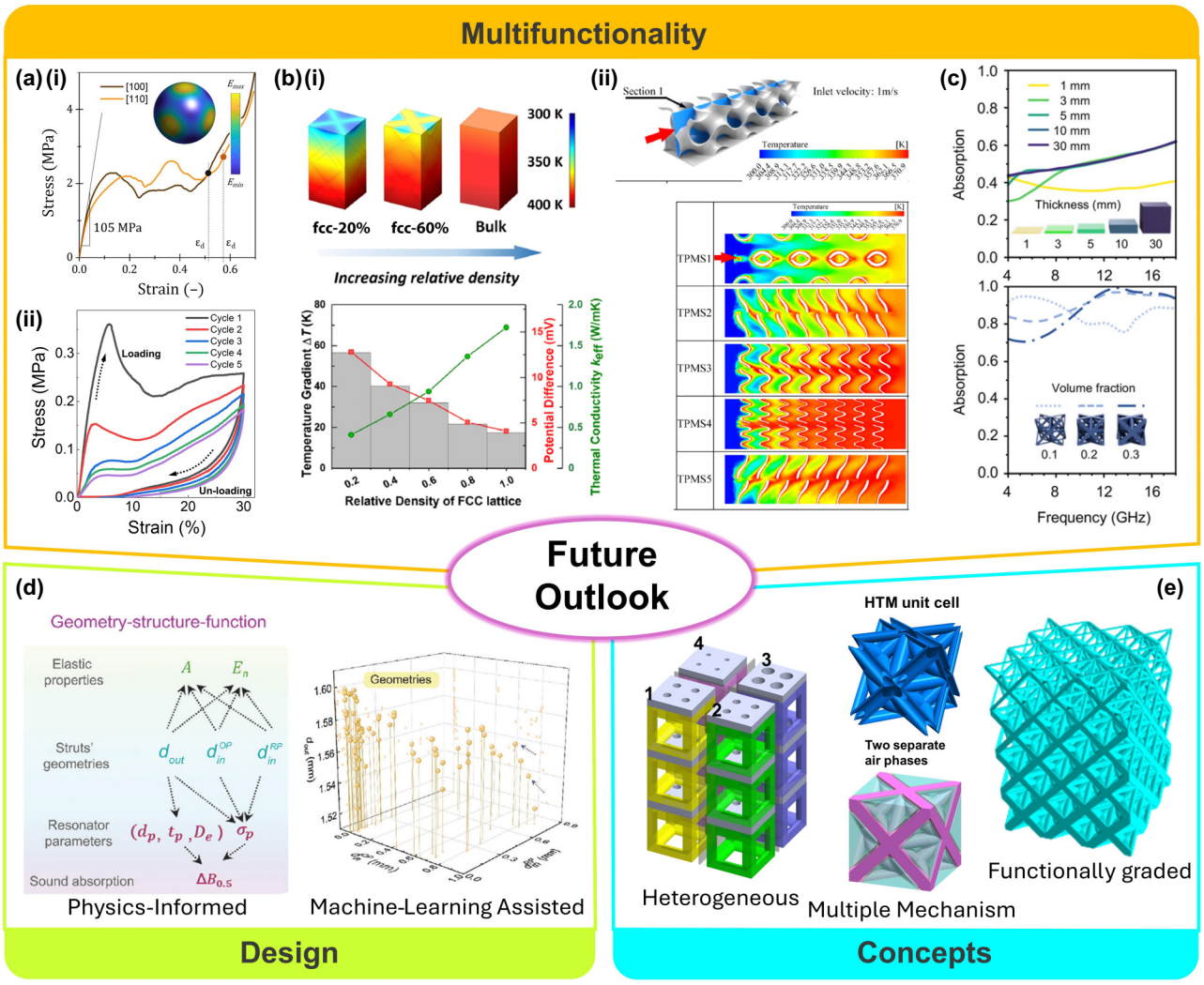


FIG. 4. The future outlook for lattice structures. (a) The potential of achieving different compressive mechanical properties in lattices, such as (i) high toughness [32] or (ii) deformation recoverability [28]. (b) The thermal properties, revealing (i) decreased thermal conductivity with increasing porosity in lattices [38] and the potential to achieve (ii) a customized rate of convective heat transfer [39]. (c) Unique electromagnetic wave properties of lattices as compared to a solid bulk material. (d) Advanced design techniques possible for the design of future lattices, including physics-informed and/or machine-learning-assisted techniques [40]. (e) Advanced design concepts for sound-insulating lattices, such as adopting heterogeneous assembly [19], integrating multiple mechanisms [41], or functionally graded design [15].

explore vast design spaces to identify geometries that achieve desired performance metrics [Fig. 4(d)] [46]. These algorithms can be trained to predict structural-property relationships or generate novel lattice topologies targeting specific sound attenuation intensity and frequency, and any other desired additional physical properties outlined in the previous section. Successes have been shown; e.g., in Refs. [40,47], the authors have successfully designed and optimized lattice structures that simultaneously achieve desired acoustic properties, sound absorption herein, and mechanical toughness. Such computational approaches can greatly reduce the expenses associated with extensive FEA or experiments, accelerating the iterative design-fabrication-testing cycle.

Further advancing the concept of multifunctionality is the exploration of hybrid lattice arrangements [Fig. 4(e)]. Instead of relying on a single lattice morphology, future designs may integrate multiple types, such as combining heterogeneously architectured lattice units, or in fact different lattices, such as plate and TPMS structures in the same framework, to achieve extended bandwidth within a single metaframework. For instance, this concept has been shown with success in sound absorption [48,49], a related acoustical property. Apart from acoustics, these hybrid architectures also allow for spatial tuning of mechanical

or thermal properties [50], enabling customized properties possible. In such cases, multiple resonance can also be achieved, such as achieving simultaneous Helmholtz, cavity, or Fabry-Perot resonance, in a single structure, to allow broadened attenuation bandwidth [33]. For lattice structures, this has been demonstrated for sound absorption. In the work of Li *et al*., a hollow-tube lattice has been demonstrated to leverage dual sound-dissipation mechanisms: one arising from Helmholtz resonance and the other from cavity-based resonance, enabled by the presence of two distinct air regions within the structure [41]. Another concept to be considered would be the introduction of functional gradings, where unit-cell geometry, density, or material composition varies gradually along the structure. For acoustics, functionally graded lattices have shown to display enhanced sound absorption compared to nongraded ones [51]. Overall, by combining the rigor of geometry-driven models with the flexibility of emerging materials and computational intelligence, future lattice metamaterials are poised to transcend traditional boundaries.

ACKNOWLEDGMENTS

X.L. acknowledges the support from Newcastle University's Research Support Allowance for this work.

DATA AVAILABILITY

The data that support the findings of this article are openly available [52].

[1] D. A. Bies, C. H. Hansen, and C. Q. Howard, *Engineering Noise Control* (CRC Press, Abingdon, 2017).
[2] L. Fredianelli, L. G. Del Pizzo, and G. Licitra, Recent developments in sonic crystals as barriers for road traffic noise mitigation, Environments **6**, 14 (2019).
[3] A. Gupta, A review on sonic crystal, its applications and numerical analysis techniques, Acoust. Phys. **60**, 223 (2014).
[4] T. Miyashita, Sonic crystals and sonic wave-guides, Meas. Sci. Technol. **16**, R47 (2005).
[5] A. Tajsham, D. Younesian, J. Goodini, and A. Hosseinkhani, A new polyhedral sonic crystal for broadband sound barriers: Optimization and experimental study, Appl. Acoust. **218**, 109881 (2024).
[6] L. Barguet, V. Romero-García, N. Jiménez, L. M. Garcia-Raffi, V. J. Sánchez-Morcillo, and J.-P. Groby, Natural sonic crystal absorber constituted of seagrass (Posidonia Oceanica) fibrous spheres, Sci. Rep. **11**, 711 (2021).
[7] R. Martínez-Sala, C. Rubio, L. M. García-Raffi, J. V. Sánchez-Pérez, E. A. Sánchez-Pérez, and J. Llinares, Control of noise by trees arranged like sonic crystals, J. Sound Vib. **291**, 100 (2006).
[8] X. Qin, A. Ni, Z. Chen, M. Fang, and Y. Li, Numerical modeling and field test of sonic crystal acoustic barriers, Environ. Sci. Pollut. Res. **30**, 16289 (2023).
[9] K. Mohapatra and D. Jena, Insertion loss of sonic crystal made with multi resonant shells, Appl. Acoust. **171**, 107676 (2021).
[10] J. Redondo, D. Ramírez-Solana, and R. Picó, Increasing the insertion loss of sonic crystal noise barriers with Helmholtz resonators, Appl. Sci. **13**, 3662 (2023).
[11] P. Ball, Rod forest cuts environmental noise, Nature **57** (2003).
[12] S. Kumar and H. P. Lee, Recent advances in acoustic metamaterials for simultaneous sound attenuation and air ventilation performances, Crystals **10**, 686 (2020).
[13] X. Zhang, Y. Wang, B. Ding, and X. Li, Design, fabrication, and mechanics of 3D micro-/nanolattices, Small **16**, 1902842 (2020).
[14] X. Li and W. Zhai, in *Materials in Advanced Manufacturing*, edited by Y. Yu and S. Zhang (CRC Press, Boca Raton, 2022).
[15] X. Li, J. W. Chua, X. Yu, Z. Li, M. Zhao, Z. Wang, and W. Zhai, 3D-printed lattice structures for sound absorption: Current progress, mechanisms and models, structural-property relationships, and future outlook, Adv. Sci. **11**, 2305232 (2024).
[16] C. Crook, J. Bauer, A. Guell Izard, C. Santos de Oliveira, J. Martins de Souza e Silva, J. B. Berger, and L. Valdevit, Plate-nanolattices at the theoretical limit of stiffness and strength, Nat. Commun. **11**, 1 (2020).
[17] X. Wang, Z. Li, J. Deng, T. Gao, K. Zeng, X. Guo, X. Li, W. Zhai, and Z. Wang, Unprecedented strength enhancement observed in interpenetrating phase composites of aperiodic lattice metamaterials, Adv. Funct. Mater. **35**, 2406890 (2025).
[18] X. Li, X. Wang, and Z. Li, Interplay between acoustical and mechanical properties in lattice structures: A geometrical perspective, Adv. Mater. Technol. **10**, 2500118 (2025).
[19] X. Li, S. Ding, X. Wang, S. L. A. Tan, and W. Zhai, Recipe for simultaneously achieving customizable sound absorption and mechanical properties in lattice structures, Adv. Mater. Technol. **10**, 2400517 (2025).
[20] T. Dixit, P. Nithiarasu, and S. Kumar, Numerical evaluation of additively manufactured lattice architectures for heat sink applications, Int. J. Therm. Sci. **159**, 106607 (2021).
[21] D. D. Lim, S. Lee, J.-H. Lee, W. Choi, and G. X. Gu, Mechanical metamaterials as broadband electromagnetic wave absorbers: Investigating relationships between geometrical parameters and electromagnetic response, Mater. Horiz. **11**, 2506 (2024).
[22] W. W. S. Ma, H. Yang, Y. Zhao, X. Li, J. Ding, S. Qu, Q. Liu, Z. Hu, R. Li, and Q. Tao, Multi-physical lattice metamaterials enabled by additive manufacturing: Design principles, interaction mechanisms, and multifunctional applications, Adv. Sci. **12**, 2405835 (2025).
[23] X. Li, Y. H. Tan, P. Wang, X. Su, H. J. Willy, T. S. Herng, and J. Ding, Metallic microlattice and epoxy interpenetrating phase composites: Experimental and simulation studies on superior mechanical properties and their mechanisms, Composites, Part A **135**, 105934 (2020).
[24] O. Al-Ketan, R. Rowshan, and R. K. A. Al-Rub, Topology-mechanical property relationship of 3D printed

strut, skeletal, and sheet based periodic metallic cellular materials, Addit. Manuf. **19**, 167 (2018).
[25] J. Berger, H. Wadley, and R. McMeeking, Mechanical metamaterials at the theoretical limit of isotropic elastic stiffness, Nature **543**, 533 (2017).
[26] X. Li, X. Yu, J. W. Chua, H. P. Lee, J. Ding, and W. Zhai, Microlattice metamaterials with simultaneous superior acoustic and mechanical energy absorption, Small **17**, 2100336 (2021).
[27] Z. Li, X. Wang, X. Li, Z. Wang, and W. Zhai, New class of multifunctional bioinspired microlattice with excellent sound absorption, damage tolerance, and high specific strength, ACS Appl. Mater. Interfaces **15**, 9940 (2023).
[28] X. Li, X. Yu, and W. Zhai, Additively manufactured deformation-recoverable and broadband sound-absorbing microlattice inspired by the concept of traditional perforated panels, Adv. Mater. **33**, 2104552 (2021).
[29] G. Li, Y. Chen, W. Chen, J. Liu, and H. He, Local resonance–Helmholtz lattices with simultaneous solid-borne elastic waves and air-borne sound waves attenuation performance, Appl. Acoust. **186**, 108450 (2022).
[30] C. Liu, J. Shi, W. Zhao, X. Zhou, C. Ma, R. Peng, M. Wang, Z. H. Hang, X. Liu, and J. Christensen, Three-dimensional soundproof acoustic metacage, Phys. Rev. Lett. **127**, 084301 (2021).
[31] O. R. Bilal, D. Ballagi, and C. Daraio, Architected lattices for simultaneous broadband attenuation of airborne sound and mechanical vibrations in all directions, Phys. Rev. Appl. **10**, 054060 (2018).
[32] X. Li, M. Zhao, X. Yu, J. W. Chua, Y. Yang, K. M. Lim, and W. Zhai, Multifunctional and customizable lattice structures for simultaneous sound insulation and structural applications, Mater. Des. **234**, 112354 (2023).
[33] N. Zhen, R.-R. Huang, S.-W. Fan, Y.-F. Wang, and Y.-S. Wang, Resonance-based acoustic ventilated metamaterials for sound insulation, npj Acoust. **1**, 1 (2025).
[34] X. Wang, H. Zhao, X. Luo, and Z. Huang, Membrane-constrained acoustic metamaterials for low frequency sound insulation, Appl. Phys. Lett. **108**, 041905 (2016).
[35] Z. Liu, X. Zhang, Y. Mao, Y. Y. Zhu, Z. Yang, C. T. Chan, and P. Sheng, Locally resonant sonic materials, Science **289**, 1734 (2000).
[36] L. Huang, Y. K. Chiang, S. Huang, C. Shen, F. Deng, Y. Cheng, B. Jia, Y. Li, D. A. Powell, and A. E. Miroshnichenko, Sound trapping in an open resonator, Nat. Commun. **12**, 4819 (2021).
[37] T. Tancogne-Dejean and D. Mohr, Stiffness and specific energy absorption of additively-manufactured metallic BCC metamaterials composed of tapered beams, Int. J. Mech. Sci. **141**, 101 (2018).
[38] D. Zhang, N. Ngoh Yen Qi, S. Faye Duran Solco, X. Li, and A. Suwardi, Lattice architectures for thermoelectric energy harvesting, ACS Energy Lett. **9**, 2240 (2024).
[39] A. Barakat and B. Sun, Enhanced convective heat transfer in new triply periodic minimal surface structures: Numerical and experimental investigation, Int. J. Heat Mass Transfer **227**, 125538 (2024).
[40] Z. Li, K. Zeng, Z. Guo, Z. Wang, X. Yu, X. Li, and L. Cheng, All-in-one: An interwoven dual-phase strategy for acousto-mechanical multifunctionality in microlattice metamaterials, Adv. Funct. Mater. **35**, 2420207 (2025).
[41] X. Li, X. Yu, and W. Zhai, Less is more: Hollow-truss microlattice metamaterials with dual sound dissipation mechanisms and enhanced broadband sound absorption, Small **18**, 2204145 (2022).
[42] R. Ju, G. Xu, L. Xu, M. Qi, D. Wang, P. C. Cao, R. Xi, Y. Shou, H. Chen, and C. W. Qiu, Convective thermal metamaterials: Exploring high-efficiency, directional, and wave-like heat transfer, Adv. Mater. **35**, 2209123 (2023).
[43] Q. An, D. Li, W. Liao, T. Liu, D. Joralmon, X. Li, and J. Zhao, A novel ultra-wideband electromagnetic-wave-absorbing metastructure inspired by bionic gyroid structures, Adv. Mater. **35**, 2300659 (2023).
[44] X. Xia, C. M. Spadaccini, and J. R. Greer, Responsive materials architected in space and time, Nat. Rev. Mater. **7**, 683 (2022).
[45] C. C. Wu, S. C. Loke, Z. Lu, M. Shrestha, B. C. Khoo, and G. K. Lau, Transformation from Helmholtz to membrane resonance by electro-adhesive zip of a double-layer microslit acoustic absorber, Adv. Mater. Technol. **8**, 2201757 (2023).
[46] X. Zheng, X. Zhang, T. T. Chen, and I. Watanabe, Deep learning in mechanical metamaterials: from prediction and generation to inverse design, Adv. Mater. **35**, 2302530 (2023).
[47] Z. Hu, J. Ding, S. Ding, W. W. S. Ma, J. W. Chua, X. Li, W. Zhai, and X. Song, Machine learning–enabled inverse design of shell-based lattice metamaterials with optimal sound and energy absorption, Virtual Phys. Prototyping **19**, e2412198 (2024).
[48] J. W. Chua, W. Zhai, and X. Li, Elucidating structure-property relationships for optimization of plate lattice sound absorbers, Mater. Des. **253**, 113801 (2025).
[49] J. W. Chua, Z. Lai, X. Li, and W. Zhai, LattSAC: A software for the acoustic modelling of lattice sound absorbers, Virtual Phys. Prototyping **19**, e2342432 (2024).
[50] M. J. Baishya, B. J. Sahariah, N. Muthu, and P. Khanikar, Composite strut-plate lattice: A high-stiffness design of cellular metamaterial having excellent strength and energy absorption ability, Mater. Today Commun. **33**, 104939 (2022).
[51] J. Boulvert, T. Cavalieri, J. Costa-Baptista, L. Schwan, V. Romero-García, G. Gabard, E. R. Fotsing, A. Ross, J. Mardjono, and J.-P. Groby, Optimally graded porous material for broadband perfect absorption of sound, J. Appl. Phys. **126**, 175101 (2019).
[52] X. Li, Lattice metamaterials as advanced airborne sound insulators, Mendeley Data, V1, https://doi.org/10.17632/2dd82j8sf9.1.